Molecular Pharmacology Fast Forward. Published on April 24, 2018 as DOI: 10.1124/mol.118.111633
This article has not been copyedited and formatted. The final version may differ from this version.

Assessment of the molecular mechanisms of action of novel 4-phenylpyridine-2-one and 6-phenylpyrimidin-4-one allosteric modulators at the M_1 muscarinic acetylcholine receptors.

Emma T van der Westhuizen, Arthur Spathis, Elham Khajehali, Manuela Jörg, Shailesh N Mistry, Ben Capuano, Andrew B Tobin, Patrick M Sexton, Peter J Scammells, Celine Valant and Arthur Christopoulos

Drug Discovery Biology, Monash Institute of Pharmaceutical Sciences, Monash University, 381 Royal Parade, Parkville, Victoria 3052, Australia (ETvdW, AS, EK, PMS, CV, AC)

Medicinal Chemistry, Monash Institute of Pharmaceutical Sciences, Monash University, 381 Royal Parade, Parkville, Victoria 3052, Australia (MJ, SNM, BC, PS)

Centre for Biomolecular Sciences, University of Nottingham, University Park, Nottingham NG7 2RD, United Kingdom (SNM)

Centre for Translational Pharmacology, Institute of Molecular, Cell and Systems Biology, College of Medical, Veterinary and Life Sciences, University of Glasgow, Glasgow, G12 8QQ, United Kingdom (ABT)

Molecular Pharmacology Fast Forward. Published on April 24, 2018 as DOI: 10.1124/mol.118.111633
This article has not been copyedited and formatted. The final version may differ from this version.

2. Running title page:

a) Running title: Characterization of novel M_1 mAChR allosteric modulators

b) Corresponding author: Prof Arthur Christopoulos
Drug Discovery Biology
Monash Institute for Pharmaceutical Sciences
381 Royal Parade, Parkville 3052 VIC
AUSTRALIA
Tel: +61 3 9903 9067
Email: Arthur.Christopoulos@monash.edu

c) Manuscript information:

Number of text pages: 41
Number of tables: 3
Number of figures: 9
Number of references: 46
Number of words in abstract: 243
Number of words in introduction: 737
Number of words in discussion: 1269

d) Non-standard abbreviations

ACh, acetylcholine; BQCA, benzyl quinolone carboxylic acid; CHO, Chinese hamser ovary; CNS, central nervous system; DMEM, Dulbecco modified eagle medium; ERK1/2, extracellular signal-regulated kinases 1/2; FBS, fetal bovine serum; GPCR, G protein-coupled receptor; HTRF. Homogenous time resolved FRET; IP_1 inositol monophosphate; mAChR, muscarinic acetylcholine receptor; MIPS1674, 4-(2-((4-(1*H*-pyrazol-4-yl)benzyl)oxy)phenyl)-1-(2-hydroxycyclohexyl)pyridin-2(1*H*)-one; MIPS1745, 1-(2-hydroxycyclohexyl)-4-(2-((6-(1-methyl-1*H*-pyrazol-4-yl)-pyridin-3-yl)methoxy)phenyl)pyridin-2(1*H*)-one; MIPS1780, 3-(2-hydroxycyclohexyl)-6-(2-((4-(1-methyl-1*H*-pyrazol-4-yl)- benzyl)oxy)phenyl)pyrimidin-4(3*H*)-one; MWC, Monod-Wyman-Changeux; NAL, neutral allosteric ligand; NAM, negative allosteric modulator; Oxo-M, oxotremorine-M; PAM, positive allosteric modulator; PBS, phosphate-buffered saline; PEI, polyethyleneimine; Rluc, *Renilla luciferase*; SF, serum-free; Xan, xanomeline; YFP, yellow fluorescent protein

Molecular Pharmacology Fast Forward. Published on April 24, 2018 as DOI: 10.1124/mol.118.111633
This article has not been copyedited and formatted. The final version may differ from this version.

Abstract

Positive allosteric modulators (PAMs) that target the M_1 muscarinic acetylcholine (ACh) receptor (M_1 mAChR) are potential treatments for cognitive deficits in conditions such as Alzheimer's disease and schizophrenia. We recently reported novel 4-phenylpyridine-2-one and 6-phenylpyrimidin-4-one M_1 mAChR PAMs with the potential to display different modes of positive allosteric modulation and/or agonism (Mistry et al., 2016), but their molecular mechanisms of action remain undetermined. The current study compared the pharmacology of three such novel PAMs with the prototypical first-generation PAM, BQCA, in a recombinant Chinese hamster ovary (CHO) cell line stably expressing the human M_1 mAChR. Interactions between the orthosteric agonists and the novel PAMs or BQCA suggested their allosteric effects were solely governed by modulation of agonist affinity. The greatest degree of positive co-operativity was observed with higher efficacy agonists, whereas minimal potentiation was observed when the modulators were tested against the lower efficacy agonist, xanomeline. Each PAM was investigated for its effects on the endogenous agonist, ACh, on three different signalling pathways, (ERK1/2 phosphorylation, IP_1 accumulation and β-arrestin-2 recruitment), revealing that the allosteric potentiation generally tracked with the efficiency of stimulus-response coupling and that there was little pathway bias in the allosteric effects. Thus, despite the identification of novel allosteric scaffolds targeting the M_1 mAChR, the molecular mechanism of action of these compounds is largely consistent with a model of allostery previously described for BQCA, suggesting that this may be a more generalized mechanism for M_1 mAChR PAM effects than previously appreciated.

Molecular Pharmacology Fast Forward. Published on April 24, 2018 as DOI: 10.1124/mol.118.111633
This article has not been copyedited and formatted. The final version may differ from this version.

Introduction

The muscarinic acetylcholine receptors (mAChRs) belong to the rhodopsin-like (Class A) family of G protein-coupled receptors (GPCRs). Five distinct mAChR subtypes (denoted M_1-M_5) exist and exhibit a widespread distribution throughout the central nervous system (CNS) and peripheral organs (Caulfield 1993; Nathanson 2008; Kruse et al., 2014). The M_1, M_3 and M_5 mAChRs preferentially couple to $G_{q/11}$ proteins, whereas the M_2 and M_4 mAChRs preferentially couple to $G_{i/o}$ proteins. However, an ever-growing array of additional signalling pathways, including those not necessarily mediated by G proteins, has also been linked to mAChR activation (Lanzafame et al., 2003).

The M_1 mAChR is highly expressed in the cerebral cortex, hippocampus, striatum and thalamus (Cortés et al., 1986; 1987; Elhert and Tran, 1990); regions vital for memory, cognitive and locomotor functions. Therefore, the M_1 mAChR has long been implicated in learning and memory, and remains a potential target for the treatment of Alzheimer's disease and schizophrenia (Caulfield 1993; Langmead et al., 2008). A role for the M_1 mAChR in treating the cognitive impairment in both of these diseases is further supported by the decrease in M_1 mAChR expression in the pre-frontal cortex in brains from schizophrenic patients (Melancon et al., 2013; Conn et al., 2009). Improved cognition, learning and memory were observed in preclinical studies using the M_1/M_4-preferring orthosteric agonist, xanomeline (Xan), which were attenuated in M_1 mAChR knockout (KO) mice (Bymaster et al., 2003), whereas memory deficits have been observed upon administration of mAChR antagonists or M_1 mAChR KO in mice (Sauerberg et al., 1992; Wess 2004; Davie et al., 2014). Importantly, Xan demonstrated clinical efficacy, particularly in treating psychosis and cognitive decline in clinical trials of Alzheimer's disease and schizophrenia. Despite this,

Molecular Pharmacology Fast Forward. Published on April 24, 2018 as DOI: 10.1124/mol.118.111633
This article has not been copyedited and formatted. The final version may differ from this version.

Xan was not pursued further due to unacceptable off-target effects, largely attributed to a lack of mAChR subtype selectivity (Bodick et al., 1997; Shekar et al., 2008).

Encouragingly, the mAChRs possess spatially distinct allosteric sites, which can be selectively targeted (Kruse et al., 2013; 2014). Recently, benzyl quinolone carboxylic acid (BQCA) was described as the first highly selective positive allosteric modulator (PAM) of the M_1 mAChR, with preclinical efficacy in animal models of cognition (Ma et al., 2009) and has served as a major impetus for new discovery efforts (Kruse et al., 2014). However, significant challenges and unanswered questions remain regarding the optimal type of allosteric ligand for successful progression through preclinical studies to man. For instance, allosteric modulators can display complex behaviours such as "probe dependence", where the magnitude and direction of an allosteric effect for the modulator can change depending on which orthosteric ligand is used as a probe for receptor function (Kenakin 2005). Another example is "biased modulation"; the ability of different allosteric ligands to engender unique receptor conformations, whereby certain signalling pathways are differentially modulated relative to others (Kenakin and Christopoulos 2013; Christopoulos 2014).

The simplest mechanism that explains allostery is the classic Monod-Wyman-Changeux (MWC) model (Monod et al., 1965), which predicts that probe dependence arises as a function of the efficacy of the orthosteric ligand, and that biased modulation cannot occur without the existence of additional active states (Canals et al., 2011; Changeux and Christopoulos 2016). A characterization of BQCA at the M_1 mAChR revealed that BQCA indeed behaves in a manner generally consistent with a two-state MWC mechanism (Canals et al., 2012; Ehlert and Griffin, 2014). However, this is not always the case with other mAChR modulators (e.g. Valant et al., 2012), and thus detailed molecular pharmacological

Molecular Pharmacology Fast Forward. Published on April 24, 2018 as DOI: 10.1124/mol.118.111633
This article has not been copyedited and formatted. The final version may differ from this version.

characterisation is a necessary first step in understanding the mechanism of action of any new allosteric ligands. Although BQCA was a major breakthrough in terms of proof of concept, it possesses a very low affinity for the receptor, and additional liabilities that precluded it from further clinical development (Canals et al., 2011; Davoren et al., 2016). Thus, there remains an ongoing need for the discovery of new M_1 mAChR PAMs.

Our laboratory recently identified a series of novel M_1 mAChR PAMs with 4-phenylpyridine-2-one and 6-phenylpyrimidin-one scaffolds that are distinct from BQCA (Mistry et al., 2016). However, a detailed mechanistic evaluation of their pharmacological properties has not been undertaken. Thus, the aim of this study was to characterise exemplar molecules from this series of PAMs and compare their behaviours to BQCA, particularly with regards to mechanisms underlying probe dependence and the potential for biased modulation. We found that, despite possessing a chemically distinct scaffold, the novel PAMs generally behave in a manner akin to that of BQCA.

Materials and Methods

Materials: Dulbecco's Modified Eagle Medium (DMEM) and FlpIn Chinese hamster ovary (CHO) cells were purchased from Invitrogen (Carlsbad, CA, USA). Fetal bovine serum was purchased from ThermoTrace (Melbourne, VIC, Australia). The IP-One assay kit and reagents were purchased from Cisbio (Codolet, France). [^{3}H]-NMS (70.0 Ci/mmol) and AlphaScreen^{TM} protein A IgG beads were purchased from Perkin Elmer Life and Analytical Sciences (Waltham, MA, USA). The *Sure-Fire*^{TM} cellular ERK1/2 assay kits were a generous gift from TGR BioSciences (Adelaide, Australia). Polyethyleneimine (PEI, molecular mass, 25kDa) was from Polysciences (Warrington, PA). 1-(4-Methoxybenzyl)-4-oxo-1,4-dihydroquinoline-3-carboxylic acid (benzyl quinolone carboxylic acid; BQCA), 4-(2-((4-(1*H*-pyrazol-4-yl)benzyl)oxy)phenyl)-1-(2-hydroxycyclohexyl)pyridin-2(1*H*)-one (MIPS1674), 1-(2-hydroxycyclohexyl)-4-(2-((6-(1-methyl-1*H*-pyrazol-4-yl)-pyridin-3-yl)methoxy)phenyl)pyridin-2(1*H*)-one (MIPS1745), and 3-(2-hydroxycyclohexyl)-6-(2-((4-(1-methyl-1*H*-pyrazol-4-yl)- benzyl)oxy)phenyl)pyrimidin-4(3*H*)-one (MIPS1780) were synthesized in house (Mistry et al. 2016). Xanomeline was a generous gift from Dr. Christian Felder (Eli Lilly, USA). Coelenterazine h was purchased from Nanolight Technologies (Pinetop, AZ, USA). The YFP-β-arrestin-2 construct was a gift from Dr. Marc Caron (Duke University). The M_1-Rluc8 constructs were generated in-house as described previously (Yeatman et al. 2014). All other chemicals were purchased from Sigma-Aldrich (St Louis, MO).

Cell culture: FlpInCHO cells stably expressing the wild type human muscarinic acetylcholine M_1 receptor (hM_1 mAChR; 37031±3397 sites/cell) (Mistry et al., 2016) were grown in DMEM (supplemented with 5% FBS), and were used for the IP_1 accumulation and ERK1/2 signaling assays. For the β-arrestin-2 recruitment assays, $3x10^6$ parental FlpInCHO

Molecular Pharmacology Fast Forward. Published on April 24, 2018 as DOI: 10.1124/mol.118.111633
This article has not been copyedited and formatted. The final version may differ from this version.

cells were transiently transfected with 0.6μg of M_1-*Renilla luciferase* (Rluc)-8, 1.8μg of YFP-β-arrestin-2 and 3.6μg of empty pcDNA vector in a 100mM dish, using linear polyethyleneimine (PEI:DNA ratio 6:1) diluted in NaCl (150mM). DNA:PEI complexes were formed by incubation at room temperature for 15 min, then added to the cells and incubated at 37°C for 24h. Transfected cells were replated into white CulturPlates (Perkin Elmer) and incubated for a further 24h prior to use in signalling assays.

IP_1 accumulation assay: The IP-one assay kit (Cisbio, France) was used for the quantitative measurement of myo-inositol 1 phosphate (IP_1). 10,000 cells/well were seeded into 96 well plates and incubated overnight at 37°C. The following day, cells were pre-incubated with IP_1 stimulation buffer (10mM HEPES, 1mM $CaCl_2$, 0.5mM $MgCl_2$, 4.2mM KCl, 146mM NaCl, 5.5mM D-glucose, 50mM LiCl, pH 7.4) for 1h at 37°C. Orthosteric and allosteric ligands were added and incubated for a further 1h at 37°C. Cells were lysed in lysis buffer (50mM HEPES-NaOH pH 7.0, 15mM KF, 1.5% (v/v) Triton-X-100) and 14μL of cell lysates were transferred into 384-well Optiplates (PerkinELmer Life Sciences). An IP_1 standard curve was prepared and added to the Optiplates in parallel. Homogenous time resolved FRET (HTRF) reagents (cryptate-labeled anti-IP_1 antibody, the d_2-labeled IP_1 analogue; diluted 1:20 in lysis buffer) were added and plates were incubated for 1h at 37°C. Samples were excited at 340nm and emission was captured at 590 and 665 nm using the Envision multi-label plate reader (PerkinElmer Life Sciences). IP_1 concentrations were interpolated from the standard curve using HTRF ratio values, and responses were normalized to the maximum response elucidated by ACh.

Receptor alkylation studies in IP_1 accumulation experiments: 10,000 cells/well were seeded into poly-D-lysine coated 96-well plates. Following the initial 1h incubation in IP_1

Molecular Pharmacology Fast Forward. Published on April 24, 2018 as DOI: 10.1124/mol.118.111633
This article has not been copyedited and formatted. The final version may differ from this version.

stimulation buffer, cells were pre-treated for 30 min at 37°C with varying concentrations of the irreversible orthosteric-site alkylating agent, phenoxybenzamine (PBZ) or vehicle control, followed by three washes with PBS. The IP_1 assay was then performed as described above.

ERK1/2 phosphorylation: The AlphaScreen-based *SureFire* kit was used for the quantitative measurement of phosphorylated ERK1/2 (pERK1/2). 25,000 cells/well were plated into 96-well plates and incubated overnight at 37°C. The following day, the growth medium was replaced with serum-free (SF) medium for 6h at 37°C, then the cells were stimulated for 5 min (peak response from time course, data not shown) with various concentrations of ACh or FBS (10% v/v) with or without different concentrations of allosteric ligands at 37°C. Cells were lysed in 100µL/well *SureFire* lysis buffer at -20°C overnight. Plates were thawed at room temperature and 10µL of the cell lysates were transferred to a 384-well Optiplate. In reduced lighting conditions, 8.5µl of detection buffer (reaction buffer/activation buffer/acceptor beads/donor beads; 60:10:0.3:0.3) was added and plates were incubated for 1h at 37°C. Fluorescence signal was measured using the Envision multilabel plate reader with AlphaScreen settings. Data were expressed as a percentage of the pERK1/2 mediated by 10% FBS or maximum ACh response.

β-arrestin-2 recruitment assays: FlpInCHO cells were transiently transfected with M_1-Rluc8 and YFP-β-arrestin-2 as described in cell culture section above. 24h later, they were replated into white 96 well Optiplates. Cells were equilibrated in Hanks' balanced salt solution for 1h at 37°C. Coelenterazine h (final concentration 5µM), was added to each well, then 5 min later various concentrations of ligands were added. Luminescence and fluorescence readings were captured 10 min after coelenterazine h addition using the LUMIstar Omega (BMG LabTech, Offenburg, Germany) that allows for the sequential integration of the signals detected at 475

Molecular Pharmacology Fast Forward. Published on April 24, 2018 as DOI: 10.1124/mol.118.111633
This article has not been copyedited and formatted. The final version may differ from this version.

± 30 and 535 ± 30 nm using filters with the appropriate band pass. Data are presented as BRET ratio, calculated as the ratio of YFP to Rluc8 signals and were normalized to the maximum possible BRET ratio elucidated by ACh.

Data analysis: All data analysis was performed using GraphPad Prism v.7.02. Concentration response curves were fitted using a three parameter logistic non-linear regression model to derive potency (pEC_{50}) and efficacy (E_{max}) parameters.

IP_1 alkylation experiments were globally fitted to an operational model of agonism (Black and Leff, 1983) to determine orthosteric agonist equilibrium dissociation constant (functional affinity; K_A) and the agonist operational efficacy (τ), which takes both receptor density and stimulus-response coupling efficiency into account:

$$E = basal + \frac{(E_m - basal)\tau^n[A]^n}{\tau^n[A]^n + ([A]+K_A)^n} \quad \text{(Eqn 1)}$$

In this model, basal is the response in the presence of vehicle, E_m is the maximum possible pathway response, [A] is the agonist concentration and *n* represents the slope of transducer function that links occupancy to response.

Concentration-response curves for the functional interactions between orthosteric and allosteric ligands were globally fitted to the following simplified operational model of allostery and agonism (Aurelio et al., 2009):

$$E = basal + \frac{(E_m - basal)([A](K_B + \alpha\beta[B] + \tau_B[B][EC_{50}])^n}{[EC_{50}]^n(K_B+[B])^n + ([A](K_B+\alpha\beta[B]) + \tau_B[B][EC_{50}])^n} \quad \text{(Eqn 2)}$$

Where basal is the response in the presence of vehicle, [B] is the concentration of allosteric ligand and K_B represents its equilibrium dissociation constants. τ_B represents an operational measure of allosteric ligand efficacy, α denotes the binding cooperativity between orthosteric

Molecular Pharmacology Fast Forward. Published on April 24, 2018 as DOI: 10.1124/mol.118.111633
This article has not been copyedited and formatted. The final version may differ from this version.

and allosteric ligand, whereas β denotes a scaling factor that quantifies the allosteric effect of the modulator on orthosteric ligand efficacy. This model assumes that all orthosteric ligands are either full agonists at the receptor on both the absence/presence of modulator and/or there is no efficacy modulation (i.e., β = 1). As shown in the Results, one or both of these assumptions were met with the various orthosteric ligands used, and thus the β parameter was constrained to 1. All other parameters are as defined in equation 1.

Also as shown in the Results, the ERK1/2 responses at the M_1 mAChR were bell-shaped. For the purposes of fitting the allosteric operational model to the data, the points defining the decreasing phases of the curves (i.e., those beyond 10μM of agonist) were removed from each curve to allow convergence of the allosteric operational model (Eqn 2).

All affinity, potency and cooperativity values were estimated as logarithms (Christopoulos 1998) and statistical comparisons between values were by one-way analysis of variance with either a Neuman-Kewls or Dunnett's multiple comparison test. A value of $p<0.05$ was considered statistically significant.

Molecular Pharmacology Fast Forward. Published on April 24, 2018 as DOI: 10.1124/mol.118.111633
This article has not been copyedited and formatted. The final version may differ from this version.

Results:

Novel 4-phenylpyridin-2-one and 6-phenylpyrimidin-4-one based compounds are selective for the M_1 mAChR over other mAChR subtypes.

Recent work from our laboratory identified a novel series of 4-phenylpyridin-2-one and 6-phenylpyrimidin-4-one M_1 mAChR PAMs (Figure 1A) that represent a different chemical scaffold to BQCA and related analogues (Mistry et al., 2016). When assessed for effects on the IP_1 signalling pathway, our preliminary pharmacological characterization indicated that MIPS1674 was an allosteric agonist with minimal PAM activity against ACh, MIPS1745 was a "pure" PAM of ACh with no direct allosteric agonism, whereas MIPS1780 behaved as a mixed PAM-agonist in modulating ACh function (akin to responses observed with BQCA). Thus, the fact that these three PAMs potentially exhibited three different "allosteric phenotypes" (Mistry et al., 2016) formed the basis for selecting them for further pharmacological evaluation. These compounds were initially tested to ensure they were selective for the M_1 mAChR over other mAChR subtypes using an ERK1/2 phosphorylation assay. Figure 1B-C shows that all PAMs modulated ACh activity at the M_1 mAChR, but no modulation of ACh-mediated ERK1/2 responses were observed for M_2, M_3, M_4, or M_5 mAChR subtypes with MIPS1674, MIPS1745, MIPS1780 or BQCA (at a concentration higher than that needed to see PAM effects at the M_1 mAChR), confirming that these modulators were selective for the M_1 mAChR. It was also noted that ACh displayed a bell-shaped concentration-response relationship for mediating ERK1/2-phosphorylation at the M_1 mAChR, both in the absence or presence of modulator (Figure 1B). Although the mechanism underlying this effect is unknown, it is not due to desensitization or a change in the time to peak ACh effect at high concentrations, based on control time course experiments (not shown).

Molecular Pharmacology Fast Forward. Published on April 24, 2018 as DOI: 10.1124/mol.118.111633
This article has not been copyedited and formatted. The final version may differ from this version.

Determination of M_1 mAChR orthosteric agonist functional affinities and intrinsic efficacies in stimulating IP_1 accumulation.

The next aim of this study was to investigate the potential for probe dependence of the novel allosteric modulators and the contribution of different degrees of intrinsic agonist efficacy to the phenomenon. mAChR agonists of variable efficacies were selected to use as orthosteric probes. Specifically, the endogenous agonist, ACh, was chosen as this represents the physiologically relevant mAChR neurotransmitter against which all putative allosteric ligands need to be tested. Oxotremorine-M (Oxo-M) was chosen, as this is commonly used as a high efficacy mAChR agonist in numerous *in vitro* and *in vivo* studies (e.g., Valant et al., 2012). Iperoxo (Ixo) was chosen as it remains the highest efficacy mAChR agonist identified to date (Langmead and Christopoulos 2013; Schrage et al., 2013), while Xanomeline (Xan) was chosen because it is a partial agonist, has a functional preference for M_1 and M_4 mAChRs over other mAChR subtypes, and had progressed into clinical trials on the basis of this selectivity (see Introduction).

Initially, the affinities and intrinsic efficacies of the orthosteric agonists were characterised using an assay of M_1 mAChR-mediated IP_1 accumulation, a classic signalling pathway downstream of activation of $G_{q/11}$-linked receptors. All orthosteric agonists increased IP_1 accumulation in our FlpInCHO-hM_1 cell line in a concentration-dependent manner. ACh, Ixo and Oxo-M were all full agonists in this assay, whereas, Xan was a weak partial agonist (with an E_{max} approx. 30% of that observed for ACh; Table 1). The functional affinities (pK_A) and operational efficacies (τ) of the othosteric probes were also determined at the M_1 mAChR by treating the cells with the irreversible alkylating agent, phenoxybenzamine (PBZ), to occlude the orthosteric site (Furchgott 1966), thus reducing the number of accessible M_1 binding sites in the FlpInCHO-hM_1 cells. Increasing levels of alkylation of the orthosteric site by PBZ

Molecular Pharmacology Fast Forward. Published on April 24, 2018 as DOI: 10.1124/mol.118.111633
This article has not been copyedited and formatted. The final version may differ from this version.

substantially reduced the E_{max} of all agonists with minimal effects on the potency of ACh, Oxo-M and Xan (Figure 2). Small, albeit significant ($p < 0.05$) effects were observed on the potency of Ixo, where a 0.5-1 log unit shift was observed when treated with the higher concentrations of PBZ (1μM and 10μM, respectively). Overall, this suggests that this system has a low level of receptor reserve for this pathway in our cell line. The family of curves for each agonist was globally fitted to an operational model of agonism (Eqn 1), with the efficacy parameter, τ, allowed to vary for each curve (since τ is determined by receptor density) but all other parameters constrained to be shared. The resulting agonist functional affinity values, determined as equilibrium dissociation constants (K_A), and the τ values for the control curve (absence of PBZ) are listed in Table 1, which confirms a rank order of efficacies of Ixo ($\tau = 10.7$) > Oxo-M ($\tau = 4.6$) > ACh ($\tau = 3.6$) >> Xan ($\tau = 0.5$). In addition to the efficacy estimates, the agonist K_A values revealed that Xan and Ixo had significantly higher affinities for the M_1 mAChR than ACh or Oxo-M ($p < 0.05$, Table 1).

BQCA exhibits probe dependence with different orthosteric agonists at the M_1 mAChR.

As outlined in the Introduction, the simplest mechanism to explain probe dependence is the classic two-state MWC model. This model predicts that the effect of a PAM is to positively modulate the activity of an orthosteric agonist but negatively modulate the activity of an orthosteric antagonist (inverse agonist) in a manner that tracks with the intrinsic efficacy of the orthosteric ligand, i.e., higher efficacy agonists will be potentiated to a greater degree than lower efficacy agonists; the model does not predict pathway-biased modulation without incorporation of additional receptor states (Canals et al., 2012; Christopoulos 2014; Ehlert and Griffin, 2014). Thus, the next series of experiments investigated the potential for probe dependence between different agonists and the prototypical M_1 mAChR PAM, BQCA.

Molecular Pharmacology Fast Forward. Published on April 24, 2018 as DOI: 10.1124/mol.118.111633
This article has not been copyedited and formatted. The final version may differ from this version.

Figure 3 shows the results of interaction experiments between increasing concentrations of BQCA and each of the orthosteric agonists ACh, Oxo-M, Ixo or Xan in the IP_1 accumulation assay. BQCA did not affect the E_{max} of any orthosteric agonist tested, but did potentiate the effects of ACh on IP_1 signal transduction. The data were globally fitted to an operational model of allostery (Eqn 2), where the pK_B of the allosteric modulator, BQCA, was constrained to 4.78 (Mistry et al., 2016). This constraint was used to aid model convergence, and was selected because it is the binding affinity value determined from full interaction equilibrium binding assays between ACh, BQCA and ^{3}H-NMS in the same cell line used for this study (Mistry et al., 2016). The resulting parameter values are listed in Table 2. From these experiments and resulting analysis, two important findings were made. First, the degree of potentiation of each agonist by BQCA was variable (α values), clearly indicating probe dependence. Second, it was of note that the allosteric modulation was manifested only on the potency of each agonist (i.e., changing the EC_{50} and not on the E_{max}). Given that the prior alkylation studies (Figure 2, Table 1) confirmed that this assay has minimal receptor reserve, any potential allosteric effects on agonist signalling efficacy would have been revealed as increases in the E_{max}, at least for the lower efficacy agonists. The fact that this was not observed in any instance indicates that BQCA modulates only the affinity of the orthosteric agonists, not their efficacy. As such, the co-operativity estimates ($\alpha\beta$) from the operational model analysis are measures of "pure" affinity modulation (α).

As summarized in Table 2 and Figure 3, BQCA potentiated ACh (α_{ACh} = 40) and Ixo (α_{Ixo} = 25) to the greatest extent; Oxo-M (α_{OxoM} = 10) was potentiated to a lesser extent, although realistically these differences in potentiation were marginal, showing only a four-fold difference at most. BQCA showed no modulation, i.e., was a neutral allosteric ligand (NAL),

Molecular Pharmacology Fast Forward. Published on April 24, 2018 as DOI: 10.1124/mol.118.111633
This article has not been copyedited and formatted. The final version may differ from this version.

with respect to the weakest agonist, Xan. On its own, BQCA showed very little to no intrinsic efficacy (τ_B = 0.2-0.8), confirming previous findings (Yeatman et al., 2014).

Effects of novel M_1 mAChR PAMs on ACh-mediated IP_1 accumulation

We next investigated the effects of each of the two 4-phenylpyridin-2-one-based (MIPS1674 and MIPS1745) and the 6-phenylpyrimidin-4-one-based (MIPS1780) analogues on IP_1 accumulation mediated by the endogenous agonist, ACh (Figure 4). As observed with BQCA, each of the novel M_1 mAChR PAMs enhanced only the potency of ACh. As above, the allosteric modulator affinity values were constrained to the binding affinity values (pK_B) for MIPS1674 (4.45), MIPS1745 (4.50) and MIPS1780 (4.88) that were previously determined by Mistry et al. (2016) in full binding interaction studies in the same cell line as used in this study. The resulting co-operativity estimates (α_{ACh}) are shown in Table 2 and Figure 6. The ACh response was potentiated to a greater extent by MIPS1780 (α_{ACh} = 302) and MIPS1745 (α_{ACh} = 129) than BQCA (α_{ACh} = 40), whereas MIPS1674 (α_{ACh} = 11) clearly showed a substantially lower degree of potentiation. Interestingly, we also noted a number of differences in the behaviour of the novel PAMs compared to our initial preliminary characterization (Mistry et al., 2016). For instance, MIPS1674 showed modest modulatory effects on ACh but little to no direct allosteric agonism. MIPS1745 was not a "pure" PAM as originally described by Mistry et al., (2016) but rather, a PAM-agonist (τ_B = 1.2) like MIPS1780 (τ_B = 5.9). Although the same cellular background was used for both the current study and that of Mistry et al. (2016), the IP_1 accumulation assay protocol was performed under different conditions (adherent vs suspended cells), which may account for the differences observed.

Molecular Pharmacology Fast Forward. Published on April 24, 2018 as DOI: 10.1124/mol.118.111633
This article has not been copyedited and formatted. The final version may differ from this version.

Investigation of mechanisms of probe dependence mediated by MIPS1674, MIPS1780 and MIPS1745 with different agonists at the M_1 mAChR.

To determine whether the novel PAMs exhibit probe dependence, the interaction experiments were extended to include the effects of other mAChR agonists on IP_1 accumulation. As observed with BQCA, no effect of the novel PAMs on the maximal response of the various agonists used in this study was detected (Figure 5), again suggesting that any allosteric modulation by the novel M_1 mAChR PAMs is manifested at the level of agonist binding affinity only. Subsequent analysis of these data by an operational model of allostery (Eqn 2) provided co-operativity estimates for individual modulators with each agonist (Table 2; summarized Figure 6B-D). MIPS1674 potentiated the ACh response (α = 11) to a greater extent than Oxo-M (α = 5) and significantly more than that seen with Ixo (α = 3), suggesting that this modulator exhibits probe dependence, modulating the endogenous agonist ACh to a greater extent than the higher potency agonist Ixo. MIPS1745 and MIPS1780 behaved like BQCA, in that they potentiated ACh, Ixo and Oxo-M to similar extents (Figure 6). Xan was weakly modulated (α = 19) by the most robust PAM, MIPS1780, although the co-operativity estimate was associated with a larger error than for the other agonists. No modulation of the Xan response was observed with any of the other allosteric modulators tested, again consistent with a NAL effect. Nonetheless, the overall findings are broadly consistent with those seen with BQCA, that is, the higher efficacy agonists were modulated to a greater extent than the lowest efficacy agonist (Xan). For a weak PAM, i.e., MIPS1674, the overall degree of positive modulation was low irrespective of the agonist (Figure 6B), whereas for the most robust PAMs, i.e., MIPS1780 and MIPS1745, the magnitude of the positive cooperativity noted with ACh, Oxo-M or Ixo (Figure 6) was in the range observed with the prototypical PAM, BQCA.

Molecular Pharmacology Fast Forward. Published on April 24, 2018 as DOI: 10.1124/mol.118.111633
This article has not been copyedited and formatted. The final version may differ from this version.

Novel M_1 PAMs show minimal evidence of biased modulation

It is not uncommon to see different overall degrees of functional PAM effects of GPCR modulators in cell-based assays. Although this may be taken as presumptive evidence of "pathway biased modulation", a simpler explanation is that assays characterized by stronger stimulus-response coupling (e.g., more amplified responses), may be more prone to manifesting stronger PAM effects due to the potential greater sensitivity of PAM-agonism being unmasked in such assays (Keov et al., 2011). It is only when this property is not a contributor that true pathway bias can be considered. Previously, BQCA showed no bias, relative to ACh, when tested against carbachol in a range of signalling assays (Canals et al., 2012; Yeatman et al., 2014). To confirm this general effect we used the endogenous agonist, ACh, and the PAM, BQCA, as comparators for the effects of the new chemotypes. We first examined the effect of BQCA on the endogenous agonist, ACh, toward 3 signalling pathways; ERK1/2 phosphorylation as a representative of an efficiently coupled pathway; IP_1 accumulation and β-arrestin-2 recruitment (βarr2) as weakly coupled pathways. In Figure 7A-C, the family of curves were globally fitted to the operational model of allostery (Eqn 2), constraining the pK_B values to the binding affinity values determined by Mistry et al., (2016), as described above, and with the resulting parameters shown in Table 3. The rank order of co-operativity for the pathways was ERK1/2 (α = 871) >> IP_1 (α = 40) ≥ βarr2 (α = 23).

The novel 4-phenylpyridin-2-ones and 6-phenylpyrimidin-4-one were also tested on the same three pathways and the data sets were analysed in the same manner as BQCA (described above). MIPS1745 and MIPS1780 had the greatest efficacy (τ_B) toward the more amplified ERK1/2 pathway and lower efficacy toward the IP_1 and βarr2 pathways (Figure 8H-I, Figure 9). MIPS1780 strongly potentiated (α_{ERK} = 550; α_{IP1} = 309; $\alpha_{\beta arr2}$ = 229) all pathways. A similar pattern of potentiation was seen with MIPS1745 (α_{ERK} = 380; α_{IP1} = 129; $\alpha_{\beta arr2}$ = 42)

Molecular Pharmacology Fast Forward. Published on April 24, 2018 as DOI: 10.1124/mol.118.111633
This article has not been copyedited and formatted. The final version may differ from this version.

(Table 3, Figure 8 and Figure 9). The rank order of co-operativity was ERK1/2>IP_1>βarr2, thus as observed with BQCA, MIPS1745 and MIPS1780 were PAMs toward all pathways, and the potentiation of the responses tracked with stimulus coupling.

When the MIPS1674 data were analysed using the operational model of allostery (Eqn 2), it did not appear to modulate βarr2 recruitment, but did weakly modulate the other signalling pathways. As shown in Figure 8, Figure 9 and Table 3, MIPS1674 had weak efficacy toward the ERK1/2 (τ_B = 1.4) pathway and no efficacy for the IP_1 or βarr2 pathways. MIPS1674 weakly modulated ACh activity toward ERK1/2 and IP_1, with a rank order of co-operativity of IP_1 (α = 12) > ERK1/2 (α = 4). By visual inspection of the concentration response curves, MIPS1674 acted as a "pure" PAM towards IP_1, is an allosteric agonist with minimal PAM activity toward ERK1/2, and was a NAL toward βarr2. Although, these results may suggest that MIPS1674 has the potential to be a biased modulator at the M_1 mAChR, a more parsimonious explanation is that the low level of receptor expression and differences in stimulus-response coupling the IP_1 and β-arrestin recruitment pathway resulted in an insufficient response window to reveal any potentiation of the ACh β-arrestin recruitment response, particularly since MIPS1674 was the least effective PAM of the new series.

Molecular Pharmacology Fast Forward. Published on April 24, 2018 as DOI: 10.1124/mol.118.111633
This article has not been copyedited and formatted. The final version may differ from this version.

Discussion:

The discovery of BQCA ushered in a new era of drug discovery for the M_1 mAChR, particularly with regards to novel potential modalities for treatment of cognitive deficits (Ma et al., 2009; Davie et al., 2013). Subsequent detailed pharmacological characterization of BQCA also revealed key features consistent with the simplest mechanism of receptor allostery, namely the two-state MWC model (Canals et al., 2012), and thus provided a guide for the subsequent pharmacological assessment of novel allosteric modulators at both mAChRs and other GPCRs. This is relevant to the current study, which investigated novel PAMs chemically distinct from BQCA. Preliminary findings with the 4-phenylpyridin-2-ones and 6-phenyl-4-ones suggested that they may have diverse pharmacological phenotypes, reflective of more complex, and potentially biased, allosteric behaviours (Mistry et al., 2016). The main findings of this study indicate that the novel M_1 mAChR PAMs display probe dependence at the M_1 mAChR but minimal evidence of biased modulation. These findings have implications for future elaboration of this new chemical series, with an ultimate aim towards producing molecules that are more tractable to "drug-like" behaviour than BQCA.

As indicated previously, the key prediction of a two-state MWC model is that the degree of allosteric modulation will "track" with the efficacy of the orthosteric probe, i.e., if an allosteric ligand prefers an active receptor state, it follows that: (i) it will be a PAM of agonists and a NAM (negative allosteric modulator) of inverse agonists (and vice versa for modulators that prefer the inactive state); (ii) that higher efficacy agonists will be potentiated by PAMs to a greater extent than lower efficacy agonists; (iii), there should be no pathway-biased modulation (Canals et al., 2011; 2012). Any divergence from this behaviour could suggest a more complex mode of action involving multiple receptor states. However, since cellular stimulus-response coupling will have an effect on observed agonism (Keov et al.,

2011), it is vital to account for this property and, where possible, apply approaches that divorce the host system-dependence of allostery and agonism from the underlying molecular parameters that govern these phenomena. The different degree of maximal agonist responsiveness observed in the IP_1 accumulation assays indicated that our recombinant cell line likely exhibited a very low receptor reserve, which was confirmed by receptor alkylation experiments and application of an operational model of agonism. However, it should be noted that a detailed analysis of the predictions of the MWC model in operational terms by Ehlert and Griffin (2014) found that the only aspects of the stimulus-response transduction mechanism that should affect observed modulation (αβ values) are receptor-proximal events, e.g., receptor or transducer stoichiometry. Moreover, low efficacy agonists may be expected to show changes in the maximal response (Ehlert and Griffin, 2014), which was not observed in our current study (e.g., with Xan). It is possible that this reflects a divergence from an MWC mechanism or, more parsimoniously, that Xan selects for a very low activity state such that any effects on its signaling efficacy simply cannot be observed over the concentration range of PAMs utilized in our study.

The low receptor reserve of the FlpInCHO-hM_1 cell system proved both advantageous and, to some extent, disadvantageous depending on the question that was asked. An advantage of the low receptor reserve system is that the lack of effect of BQCA and the novel PAMs on agonist E_{max}, while modulating potency, could only be explained if the modulators mediated their effects purely through changing agonist affinity, as efficacy effects would manifest as a change in E_{max}, particularly for Xan. This allowed the application of a simplified operational model of allostery that quantified the global cooperativity of the PAMs (Aurelio et al., 2009). Although differences were observed in the behaviours and operational model parameter estimates in our IP_1 accumulation studies versus those performed by Mistry et al. (2016), this

likely reflected variances in IP_1 assay protocol, as well as potential variability in cell background due to cell passage. Irrespective, our analysis suggested that all novel PAMs, like BQCA, tended to potentiate higher efficacy agonists to a greater extent than the low efficacy agonist, Xan.

A possible disadvantage of the low receptor reserve displayed by our cell line was evident in the studies of allosteric modulation between different pathways linked to M_1 mAChR activation. Ideally, the choice of pathways was designed to reflect events that are generally considered substantially proximal (e.g., β-arrestin 2 recruitment) or substantially downstream (e.g., pERK1/2) from receptor activation, with IP_1 accumulation representing a pathway that would display a degree of stimulus-response coupling somewhere between the two (Lanzafame et al., 2003; Canals et al., 2012; Abdul-Ridha et al., 2014). This, in turn, would allow for a clear delineation of whether the modulation between a given agonist-modulator pair tracked with the degree of stimulus-response coupling or differed. The former scenario was generally the case when comparing the effects of the PAMs on ACh-mediated pERK1/2 to either β-arrestin 2 recruitment or IP_1 accumulation, but more equivocal when comparing ACh-mediated β-arrestin 2 recruitment to IP_1 accumulation. However, if the degree of receptor coupling efficiency to the IP_1 pathway and β-arrestin 2 recruitment pathways was similar, due to low receptor reserve, then the MWC model would predict similar degrees of potentiation at each pathway, and it is thus not surprising that the PAM effects on ACh at β-arrestin 2 recruitment or IP_1 accumulation did not display the degree of separation seen when compared to the pERK1/2 assays.

It is now established that allosteric ligands have the potential to engender multiple biologically active GPCR states (Kenakin et al., 2012; Davey et al., 2012; Wislar et al.,

2007). As a consequence, deviations from simple MWC-governed allosteric behaviour in terms of probe dependence and pathway bias have been observed at multiple GPCRs, emphasising the importance of routinely investigating these therapeutically relevant paradigms whenever characterising novel ligands (Christopoulos 2014; Price et al., 2005; Valant et al., 2012). For example, at the M_2 mAChR, the allosteric modulator, LY2033298, positively modulates the binding affinity of multiple orthosteric agonists, but has either positive or negative allosteric effects on the signalling efficacy and signalling pathway of the same agonists. Thus, functionally, LY2033298 is a PAM of Oxo-M, a NAL of ACh, and a NAM of Xan (Valant et al., 2012). This type of probe dependence cannot be reconciled within a two-state mechanism, and is clearly suggestive of biased modulation involving multiple receptor active states (Christopoulos 2014). Given that surrogate orthosteric probes are often used preclinically *in vitro* or *in vivo*, due to the metabolic instability of the endogenous GPCR agonist (Leach et al., 2010), or that multiple endogenous ligands and their metabolites exist for a single GPCR (van der Westhuizen et al., 2015, Wootten et al., 2012), a lack of appreciation of the differences underlying probe dependence as a function of intrinsic efficacy (i.e., simple two-state MWC model) or probe dependence as a function of different conformational states (i.e., biased modulation), can lead to misinterpretation of preclinical data and thus inappropriate selection of potential allosteric drug candidates for further optimization and development.

In conclusion, despite possessing a chemically distinct scaffold, the similar molecular fingerprints of the 4-phenylpyridine-2-one and 6-phenylpyrimidin-4-one PAMs to that of BQCA suggests a similar molecular mechanism of action, and is consistent with a common binding site. This site is proposed to overlap with the "common" allosteric binding pocket located in the extracellular vestibule of mAChRs. However, additional structure-function

Molecular Pharmacology Fast Forward. Published on April 24, 2018 as DOI: 10.1124/mol.118.111633
This article has not been copyedited and formatted. The final version may differ from this version.

analyses are required to confirm this hypothesis. Perhaps more importantly, the availability of a novel chemical scaffold of known molecular properties could facilitate the development of superior M_1 mAChR PAMs with a higher likelihood of clinical translation than first generation compounds exemplified by BQCA.

Acknowledgements:

The authors would like to thank Dr. Christian Felder, Eli Lilly, for the generous gift of xanomeline.

Molecular Pharmacology Fast Forward. Published on April 24, 2018 as DOI: 10.1124/mol.118.111633
This article has not been copyedited and formatted. The final version may differ from this version.

Authorship contributions

Participated in research design: van der Westhuizen, Spathis, Valant, Christopoulos

Conducted experiments: van der Westhuizen, Spathis, Valant, Khajehali

Contributed reagents or analytical tools: Mistry, Jörg, Scammells

Performed data analysis: van der Westhuizen, Spathis, Valant, Christopoulos

Wrote or contributed to the writing of the manuscript: van der Westhuizen, Spathis, Khajehali, Jörg, Mistry, Valant, Capuano, Tobin, Sexton, Scammells, Christopoulos.

Molecular Pharmacology Fast Forward. Published on April 24, 2018 as DOI: 10.1124/mol.118.111633
This article has not been copyedited and formatted. The final version may differ from this version.

References:

Abdul-Ridha, A., Lane, J.R., Mistry, S.N., Lopez, L., Sexton, P.M., Scammells, P.J., Christopoulos, A., and Canals, M. (2014). Mechanistic insights into allosteric structure-function relationships at the M1 muscarinic acetylcholine receptor. *J Biol Chem* **289**: 33701-33711.

Aurelio, L., Valant, C., Flynn, B.L., Sexton, P.M., Christopoulos, A., and Scammells, P.J. (2009). Allosteric modulators of the adenosine A1 receptor: synthesis and pharmacological evaluation of 4-substituted 2-amino-3-benzoylthiophenes. *J Med Chem* **52**: 4543-4547.

Black, J.W., and Leff, P. (1983). Operational models of pharmacological agonism. *Proc R Soc Lond **B** Biol Sci* **220**: 141-162.

Bodick, N.C., Offen, W.W., Levey, A.I., Cutler, N.R., Gauthier, S.G., Satlin, A., Shannon, H.E., Tollefson, G.D., Rasmussen, K., Bymaster, F.P., et al. (1997). Effects of xanomeline, a selective muscarinic receptor agonist, on cognitive function and behavioral symptoms in Alzheimer disease. *Arch Neurol* **54**: 465-473.

Bymaster, F.P., McKinzie, D.L., Felder, C.C., and Wess, J. (2003). Use of M1-M5 muscarinic receptor knockout mice as novel tools to delineate the physiological roles of the muscarinic cholinergic system. *Neurochem Res* **28**: 437-442.

Canals, M., Lane, J.R., Wen, A., Scammells, P.J., Sexton, P.M., and Christopoulos, A. (2012). A Monod-Wyman-Changeux mechanism can explain G protein-coupled receptor (GPCR) allosteric modulation. *J Biol Chem* **287**: 650-659.

Canals, M., Sexton, P.M., and Christopoulos, A. (2011). Allostery in GPCRs: 'MWC' revisited. *Trends Biochem Sci* **36:** 663-672.

Caulfield, M.P. (1993). Muscarinic receptors - characterization, coupling and function. *Pharmacol Ther* **58**: 319-379.

Changeux, J.P., and Christopoulos, A. (2016). Allosteric modulation as a unifying mechanism for receptor function and regulation. *Cell* **166**: 1084-1102.

Christopoulos, A. (1998). Assessing the distribution of parameters in models of ligand-receptor interaction: to log or not to log. *Trends Pharmacol Sci* **19**: 351-357.

Christopoulos, A. (2014). Advances in G protein-coupled receptor allostery: from function to structure. *Mol Pharmacol* **86**: 463-478.

Conn, P.J., Christopoulos, A., and Lindsley, C.W. (2009). Allosteric modulators of GPCRs: a novel approach for the treatment of CNS disorders. *Nat Rev Drug Discov* **8**: 41-54.

Cortés, R., Probst, A., Tobler, H.J., Palacios, J.M. (1986). Muscarinic cholinergic receptor subtypes in the human brain. II. Quantitative autoradiographic studies. *Brain Res* **362**: 239-253.

Cortés, R., Probst, A. and Palacios, J.M. (1987). Quantitative light microscopic autoradiographic localization of cholinergic muscarinic receptors in the human brain: forebrain. *Neurosci* **20**: 65-107.

Davey, A.E., Leach, K., Valant, C., Conigrave, A.D., Sexton, P.M., and Christopoulos, A. (2012). Positive and negative allosteric modulators promote biased signaling at the calcium-sensing receptor. *Endocrinol* **153**: 1232-1241.

Davie, B.J., Christopoulos, A., and Scammells, P.J. (2013). Development of M1 mAChR allosteric and bitopic ligands: prospective therapeutics for the treatment of cognitive deficits. *ACS Chem Neurosci* **4**: 1026-1048.

Davie, B.J., Valant, C., White, J.M., Sexton, P.M., Capuano, B., Christopoulos, A., and Scammells, P.J. (2014). Synthesis and pharmacological evaluation of analogues of benzyl quinolone carboxylic acid (BQCA) designed to bind irreversibly to an allosteric site of the M (1) muscarinic acetylcholine receptor. *J Med Chem* **57**: 5405-5418.

Davoren, J.E., Lee, C.W., Garnsey, M., Brodney, M.A., Cordes, J., Dlugolenski, K., Edgerton, J.R., Harris, A.R., Helal, C.J., Jenkinson, S., et al. (2016). Discovery of the potent and selective M1 PAM-agonist *N*-[(3*R*,4*S*)-3-Hydroxytetrahydro-2*H*-pyran-4-yl]-5-methyl-4-[4-(1,3-thiazol-4-yl)benzyl]pyridine-2-carboxamide (PF-06767832): Evaluation of efficacy and cholinergic side effects. *J Med Chem* **59**: 6313-6328.

Elhert F.J. and Griffin M.T. (2014). Estimation of ligand affinity constants for receptor states in functional studies involving the allosteric modulation of G protein-coupled receptors: implications for ligand bias. *J Pharmacol Toxicol Methods* **69**: 253-729

Elhert, F.J. and Tran, L.P. (1990). Regional distribution of M1, M2 and non-M1, non-M2 subtypes of muscarinic binding sites in rat brain. *J Pharmacol Exp Ther* **255**: 1148-1157.

Furchgott, R.F. (1966). The use of b-haloalkylamines in the differentiation of receptors and in the determination of dissociation constants of receptor-agonist complexes. *Adv Drug Res* **3**: 21-55.

Kenakin, T. (2005). New concepts in drug discovery: collateral efficacy and permissive antagonism. *Nat Rev Drug Discov* **4**: 919-927.

Kenakin, T., and Christopoulos, A. (2013). Signalling bias in new drug discovery: detection, quantification and therapeutic impact. *Nat Rev Drug Discov* **12**: 205-216.

Kenakin, T., Watson, C., Muniz-Medina, V., Christopoulos, A., and Novick, S. (2012). A simple method for quantifying functional selectivity and agonist bias. *ACS Chem Neurosci* **3**: 193-203.

Keov, P., Sexton, P.M., and Christopoulos, A. (2011). Allosteric modulation of G protein-coupled receptors: a pharmacological perspective. *Neuropharmacol* **60**: 24-35.

Kruse, A.C., Kobilka, B.K., Gautam, D., Sexton, P.M., Christopoulos, A., and Wess, J. (2014). Muscarinic acetylcholine receptors: novel opportunities for drug development. *Nat Rev Drug Discov* **13**: 549-560.

Kruse, A.C., Ring, A.M., Manglik, A., Hu, J., Hu, K., Eitel, K., Hubner, H., Pardon, E., Valant, C., Sexton, P.M., et al. (2013). Activation and allosteric modulation of a muscarinic acetylcholine receptor. *Nature* **504**: 101-106.

Langmead, C.J., and Christopoulos, A. (2013). Supra-physiological efficacy at GPCRs: superstition or super agonists? *Br J Pharmacol* **169**: 353-356.

Langmead, C.J., Watson, J., and Reavill, C. (2008). Muscarinic acetylcholine receptors as CNS drug targets. *Pharmacol Ther* **117**: 232-243.

Lanzafame, A.A., Christopoulos, A., and Mitchelson, F. (2003). Cellular signaling mechanisms for muscarinic acetylcholine receptors. *Receptors Channels* **9**: 241-260.

Leach, K., Loiacono, R.E., Felder, C.C., McKinzie, D.L., Mogg, A., Shaw, D.B., Sexton, P.M., and Christopoulos, A. (2010). Molecular mechanisms of action and in vivo validation of an M4 muscarinic acetylcholine receptor allosteric modulator with potential antipsychotic properties. *Neuropsychopharmacology* **35**: 855-869.

Ma, L., Seager, M.A., Wittmann, M., Jacobson, M., Bickel, D., Burno, M., Jones, K., Graufelds, V.K., Xu, G., Pearson, M., et al. (2009). Selective activation of the M1 muscarinic acetylcholine receptor achieved by allosteric potentiation. *Proc Natl Acad Sci U S A* **106**: 15950-15955.

Melancon, B.J., Tarr, J.C., Panarese, J.D., Wood, M.R., and Lindsley, C.W. (2013). Allosteric modulation of the M1 muscarinic acetylcholine receptor: improving cognition and a potential treatment for schizophrenia and Alzheimer's disease. *Drug Discov Today* **18**: 1185-1199.

Mistry, S.N., Jorg, M., Lim, H., Vinh, N.B., Sexton, P.M., Capuano, B., Christopoulos, A., Lane, J.R., and Scammells, P.J. (2016). 4-phenylpyridin-2-one derivatives: A novel class of positive allosteric modulator of the M1 Muscarinic Acetylcholine Receptor. *J Med Chem* **59**: 388-409.

Monod, J., Wyman, J., and Changeux, J.P. (1965). On the nature of allosteric transitions: A plausible model. *J Mol Biol* **12**: 88-118.

Nathanson, N.M. (2008). Synthesis, trafficking, and localization of muscarinic acetylcholine receptors. *Pharmacol Ther* **119**: 33-43.

Price, M.R., Baillie, G.L., Thomas, A., Stevenson, L.A., Easson, M., Goodwin, R., McLean, A., McIntosh, L., Goodwin, G., Walker, G., et al. (2005). Allosteric modulation of the cannabinoid CB1 receptor. *Mol Pharmacol* **68**: 1484-1495.

Sauerberg, P., Olesen, P.H., Nielsen, S., Treppendahl, S., Sheardown, M.J., Honore, T., Mitch, C.H., Ward, J.S., Pike, A.J., Bymaster, F.P., et al. (1992). Novel functional M1 selective muscarinic agonists. Synthesis and structure-activity relationships of 3-(1,2,5-thiadiazolyl)-1,2,5,6-tetrahydro-1-methylpyridines. *J Med Chem* **35**: 2274-2283.

Schrage, R., Seemann, W.K., Klockner, J., Dallanoce, C., Racke, K., Kostenis, E., De Amici, M., Holzgrabe, U., and Mohr, K. (2013). Agonists with supraphysiological efficacy at the muscarinic M2 ACh receptor. *Br J Pharmacol* **169**: 357-370.

Shekhar, A., Potter, W.Z., Lightfoot, J., Lienemann, J., Dube, S., Mallinckrodt, C., Bymaster, F.P., McKinzie, D.L., and Felder, C.C. (2008). Selective muscarinic receptor agonist xanomeline as a novel treatment approach for schizophrenia. *Am J Psychiatry* **165**, 1033-1039.

Valant, C., Felder, C.C., Sexton, P.M., and Christopoulos, A. (2012). Probe dependence in the allosteric modulation of a G protein-coupled receptor: implications for detection and validation of allosteric ligand effects. *Mol Pharmacol* **81**: 41-52.

van der Westhuizen, E.T., Valant, C., Sexton, P.M., and Christopoulos, A. (2015). Endogenous allosteric modulators of G protein-coupled receptors. *J Pharmacol Exp Ther* **353**: 246-260.

Wess, J. (2004). Muscarinic acetylcholine receptor knockout mice: novel phenotypes and clinical implications. *Annu Rev Pharmacol Toxicol* **44**: 423-450.

Wisler, J.W., DeWire, S.M., Whalen, E.J., Violin, J.D., Drake, M.T., Ahn, S., Shenoy, S.K., and Lefkowitz, R.J. (2007). A unique mechanism of beta-blocker action: carvedilol stimulates beta-arrestin signaling. *Proc Natl Acad Sci U S A* **104**: 16657-16662.

Wootten, D., Savage, E.E., Valant, C., May, L.T., Sloop, K.W., Ficorilli, J., Showalter, A.D., Willard, F.S., Christopoulos, A., and Sexton, P.M. (2012). Allosteric modulation of endogenous metabolites as an avenue for drug discovery. *Mol Pharmacol* **82**: 281-290.

Yeatman, H.R., Lane, J.R., Choy, K.H., Lambert, N.A., Sexton, P.M., Christopoulos, A., and Canals, M. (2014). Allosteric modulation of M1 muscarinic acetylcholine receptor internalization and subcellular trafficking. *J Biol Chem* **289**: 15856-15866.

Molecular Pharmacology Fast Forward. Published on April 24, 2018 as DOI: 10.1124/mol.118.111633
This article has not been copyedited and formatted. The final version may differ from this version.

Footnotes:

a) This work was supported by National Health and Medical Research Council Program Grant [APP1055134]. AC is a Senior Principal, and PMS a Principal, Research Fellow of the National Health and Medical Research Council of Australia. CV is supported by a Future Fellowship from the Australian Research Council. ETvdW is supported by an Early Career Fellowship from the National Health and Medical Research Council of Australia.

b) This work has been presented in part at the ASCEPT-MPGPCR joint scientific meeting 2016 in Melbourne, Australia and at the GPCR workshop 2017 in Kona, Hawaii, USA.

c) Reprint requests to Arthur Christopoulos, Monash University, Drug Discovery Biology, 381 Royal Pde Parkville VIC 3052. Email: Arthur.Christopoulos@monash.edu

d) [1] SNM is currently located at the Centre for Biomolecular Sciences, University of Nottingham, University Park, Nottingham NG7 2RD, UNITED KINGDOM.

Legends for Figures:

Figure 1. Novel 4-phenylpyridine-2-ones and 6-phenylpyrimidin-4-one selectively modulate the M_1 mAChR over other mAChR subtypes. (A) The structurally novel M_1 mAChR PAMs selected for this study, MIPS1674, MIPS1745 and MIPS1780 (previously published as compounds "**14, 17** and **29**", respectively, by Mistry et al., (2016)). They were compared to the reference modulator, BQCA. (B) The 4-pheylpyridine-2-ones and 6-phenylpyrimidin-4-one based analogs all showed intrinsic efficacy and potentiation of the ERK1/2 response at the M_1 mAChR. (C) The novel PAMs or BQCA did not modulate ACh-mediated ERK1/2 phosphorylation at the M_2, M_3, M_4 or M_5 mAChR subtypes, when tested at a concentration of 10μM. Data are mean±SEM of four independent experiments performed with duplicate repeats.

Figure 2. Receptor alkylation assays identify low receptor reserve in FlpInCHO-M_1 cell lines. FlpInCHO-M_1 cells were pre-treated with different concentrations of phenoxybenzamine (PBZ) for 30 min, followed by extensive washout to reduce receptor reserve. Cells were then stimulated for 60 min with increasing concentrations of (A) ACh, (B) Ixo, (C) Oxo-M or (D) Xan. Decreases in E_{max} and minimal changes in EC_{50} values were observed with all orthosteric ligands, suggesting that the FlpInCHO-M1 cell line used in this study expressed low levels of M_1 mAChRs. Data are mean±SEM of 6 independent experiments with repeats in duplicate. Fitted curves shown are global analysis based on the operational model (Eqn 1).

Figure 3. BQCA displays probe dependence with different agonists in IP_1 accumulation. Interaction between (A) ACh, (B) Ixo, (C) Oxo-M or (D) Xan with or without increasing

Molecular Pharmacology Fast Forward. Published on April 24, 2018 as DOI: 10.1124/mol.118.111633
This article has not been copyedited and formatted. The final version may differ from this version.

concentrations of BQCA were performed in FlpInCHO-hM_1 cells at 37°C for 1h. Data are expressed as a percentage of the maximal ACh response and are the mean ± SEM of 6-15 independent experiments performed in duplicate. Fitted curves are from global analysis of datasets according to an operational model of allosterism (Eqn 2) with parameter estimates shown in Table 2.

Figure 4. The structurally novel PAMs differentially modulate ACh-induced IP_1 accumulation at the M_1 mAChR. Experiments were performed on FlpInCHO-hM_1 cells, using increasing concentrations of ACh with or without increasing concentrations of (A) MIPS1674, (B) MIPS1745 or (C) MIPS1780 at 37°C for 1h. Data are expressed as a percentage of maximum ACh response and are the mean ± SEM of 15 independent experiments performed in duplicate. Fitted curves are from global analysis of datasets according to an operational model of allosterism (Eqn 2), with parameter estimates shown in Table 2.

Figure 5. The novel M_1 PAMs modulate IP_1 accumulation with different orthosteric probes to different extents. IP_1 accumulation assays in FlpInCHO-hM_1 cells were performed with increasing concentrations of different orthosteric probes (A, D, G) Ixo, (B, E, H) Oxo-M or (C, F, I) Xan at 37°C for 1h. Allosteric modulators (A, B, C) MIPS1674, (D, E, F) MIPS1745 and (G, H, I) MIPS1780 were co-added with the orthosteric ligands for 1h at 37°C. Curves represent the best global fit to the allosteric operational model (Eqn 2) with the resulting parameters found in Table 2. Data are mean±SEM of 6 independent experiments with repeats in duplicate.

Molecular Pharmacology Fast Forward. Published on April 24, 2018 as DOI: 10.1124/mol.118.111633
This article has not been copyedited and formatted. The final version may differ from this version.

Figure 6. Probe-dependence between orthosteric agonists and allosteric modulators. Co-operativity estimates (log α) were derived from global analysis of data sets in Figures 4 and 5 and resulting parameters are reported in Table 2. (A) BQCA potentiated ACh and Ixo more than Oxo-M. (B) MIPS1674 potentiated ACh to a greater extent than Ixo or Oxo-M. (C) MIPS1745 potentiated ACh, Ixo and Oxo-M to similar extents. (D) MIPS1780 potentiated ACh, Ixo and Oxo-M to a greater extent than Xan. Data are mean±SEM of 6-15 independent experiments with repeats in duplicate. Data were analyzed by One-way ANOVA with a Neuman-Kewls multiple comparison test, where $*p<0.05$ was considered significantly different.

Figure 7. BQCA potentiates ACh at three distinct signaling pathways. FlpInCHO-hM_1 cells were stimulated with different concentrations of ACh and responses to three different signaling pathways were measured. β-arrestin 2 recruitment and ERK1/2 responses were measured after 5 min of stimulation, whereas IP_1 accumulation was measured after 1h. BQCA potentiates ACh signaling toward (A) β-arrestin 2 recruitment, (B) IP_1 accumulation and (C) ERK1/2 phosphorylation. Data were fitted with the allosteric operational model with the resulting parameters reported in Table 3. Data are mean±SEM of 6-15 independent experiments with repeats in duplicate.

Figure 8. Minimal evidence for pathway biased modulation by the novel M_1 PAM scaffolds. FlpInCHO-hM_1 cells were stimulated with different concentrations of ACh and responses to three different signaling pathways were measured. β-arrestin 2 recruitment and ERK1/2 responses were measured after 5 min of stimulation and IP_1 accumulation was measured after 1h. MIPS1674 acted as a neutral allosteric ligand toward (A) β-arrestin 2 recruitment, as a "pure" PAM for (D) IP_1 accumulation and an allosteric agonist with

Molecular Pharmacology Fast Forward. Published on April 24, 2018 as DOI: 10.1124/mol.118.111633
This article has not been copyedited and formatted. The final version may differ from this version.

minimal PAM activity towards (G) ERK1/2 signalling. MIPS1745 and MIPS1780 were PAM-agonists toward (B and C) β-arrestin 2 recruitment, (E and F) IP_1 accumulation and (H and I) ERK1/2 phosphorylation, suggesting that they are not biased modulators of ACh at the M_1 mAChR. Fitted curves are from global analysis of datasets according to an operational model of allosterism (Eqn 2), with parameter estimates shown in Table 3. Data are mean±SEM of 4-15 independent experiments with repeats in duplicate.

Figure 9. Comparison of the efficacy and co-operativity estimates of the 4-phenylpyridin-2-one and 6-phenylpyrimidin-4-one PAMs toward three signaling pathways. FlpInCHO-hM_1 cells were stimulated with different concentrations of ACh and responses to three different signaling pathways were measured. ERK1/2 phosphorylation and β-arrestin 2 recruitment were measured after 5 min stimulation at 37°C. IP_1 accumulation was measured following stimulation with ligands for 1h at 37°C. Data from interaction experiments between different concentrations of ACh and PAMs were fitted to the operational model of allosterism (Eqn 2) and the (A, C, E, G) efficacy (log τ_B) and (B, D, F, H) cooperativity (log α) parameters were obtained (also shown in Table 3). Data are mean±SEM of 4-8 independent experiments with repeats in duplicate. Data were analysed by one-way ANOVA, with Neuman-Kewls multiple comparisons tests, where $*p<0.05$ was considered to be significantly different.

Molecular Pharmacology Fast Forward. Published on April 24, 2018 as DOI: 10.1124/mol.118.111633
This article has not been copyedited and formatted. The final version may differ from this version.

Tables:

Table 1. Empirical and operational model parameter estimates for the orthosteric ligands in mediating the IP_1 accumulation via activation of the M_1 mAChR in FlpInCHO-hM1 cells. Concentration response curves for orthosteric ligands were established in the absence or presence of PBZ pretreatment (followed by extensive washout). Data were fitted using the operational model (Eqn 1) to determine the functional affinity (pK_A) and operational efficacy ($\log\tau$) values. Parameter values are the mean±SEM of 8 independent experiments with repeats in duplicate. Data were analyzed by one way ANOVA (with alpha = 0.01) using a Dunnett's multiple comparisons test, where $*p<0.05$ was considered to be significantly different to those of the endogenous agonist ACh.

Ligand	pEC_{50}[a]	E_{max}[b]	pK_A[c]	$\log\tau_A$[d]	τ_A[e]
ACh	5.79±0.07	99.7±2.9	5.26±0.23	0.55±0.29	3.6
Ixo	7.97±0.09*	101.3±3.3	6.99±0.17*	1.03±0.23*	10.7
Oxo-M	6.08±0.13	90.3±4.8	5.35±0.28	0.66±0.40*	4.6
Xan	6.96±0.21*	29.8±2.7*	6.48±0.51*	-0.31±1.3*	0.5

[a]Negative logarithm of the EC_{50} value of the vehicle-pretreated control curve.

[b]Maximal agonist response under the vehicle-pretreated conditions, relative to ACh

[c]Negative logarithm of the functional affinity value constant K_A, derived using Eqn 1.

[d]Logarithm of the operational efficacy parameter for the orthosteric agonist in the absence of PBZ-pretreatment derived using Eqn 1.

[e]Antilogarithm of the operational efficacy parameter.

Table 2. Allosteric model estimates for 4-phenylpyridine-2-ones and 6-phenylpyrimidin-4-ones at the M_1 mAChR with different mAChR othosteric agonists for IP1 accumulation in FlpInCHO-hM1 cells. Orthosteric agonist concentration-response curve families in the absence or presence of each modulator were analysed using Eqn 2, with the logK_B constrained to the value derived previously in Mistry et al., (2016). Data are the mean±SEM of 4-15 independent experiments with repeats in duplicate. Data were analyzed by one-way ANOVA with a Neuman-Kewls multiple comparison test, where *p<0.05 was considered to be significantly different to ACh.

	BQCA				MIPS1674				MIPS1745				MIPS1780			
	logα[a]	(α)[b]	logτ_B[c]	(τ_B)[d]	logα[a]	(α)[b]	logτ_B[c]	(τ_B)[d]	logα[a]	(α)[b]	logτ_B[c]	(τ_B)[d]	logα[a]	(α)[b]	logτ_B[c]	(τ_B)[d]
ACh	1.60±0.09	(40)	-0.46±0.12	(0.3)	1.06±0.08	(11)	-3	(0)	2.11±0.12	(129)	0.08±0.05	(1)	2.48±0.14	(302)	0.77±0.04	(6)
Ixo	1.40±0.14	(25)	-0.09±0.10	(0.8)	0.44±0.17*	(3)	-3	(0)	1.86±0.17	(72)	0.10±0.07	(1)	2.22±0.17	(166)	0.87±0.05	(7)
Oxo-M	0.99±0.18*	(10)	-0.75±0.33	(0.2)	0.69±0.15	(5)	-3	(0)	1.86±0.22	(72)	-0.14±0.12	(0.7)	1.98±0.17	(95)	0.78±0.04	(6)
Xan	NM		NM		NM		NM		1	(129)	0.38±0.05*	(2)	1.29±0.62	(19)	1.16±0.07*	(14)

NM; no modulation (NAL effect)

[a]Logarithm of the functional cooperativity estimate between the orthosteric ligand and allosteric modulator derived using Eqn 2.

[b]Antilogarithm of the functional cooperativity estimate between the orthosteric ligand and allosteric modulator

[c]Logarithm of the operational efficacy parameter of the allosteric modulator derived using Eqn 2. Where no intrinsic efficacy of the allosteric modulator was observed, the τ_B values were constrained to -3 (τ = 0.001) to aid model convergence.

[d]Antilogarithmhm of the operational efficacy parameter of the allosteric modulator

Table 3. ACh potency and allosteric model parameter estimates for interaction with 4-phenylpyridine-2-ones and 6-phenylpyrimidin-4-ones at the M_1 mAChR for three different signaling pathways in FlpInCHO-hM1 cells. For allosteric model analysis, ACh concentration-response curves, established in the absence or presence of each modulator, were fitted to Eqn 3. The initial increase in ERK1/2 phosphorylation data was used (with the decreasing phase removed) for the purpose of the ERK1/2 analysis. Data are the mean±SEM of 4-15 independent experiments with repeats in duplicate. Data were analyzed by one-way ANOVA with a Newman-Keuls post hoc test to compare all groups. Results of the statistical tests are shown in Figure 9.

	BQCA			MIPS1674			MIPS1745			MIPS1780		
	ERK1/2	**IP1**	**βarr2**	**ERK1/2**	**IP1**	**βarr2**	**ERK1/2**	**IP1**	**βarr2**	**ERK1/2**	**IP1**	**βarr2**
pEC_{50}[a]	7.19±0.13	5.73±0.05	5.50±0.07	7.54±0.11	5.81±0.08	5.17±0.07	7.16±0.08	5.67±0.08	5.28±0.13	7.24±0.08	5.47±0.09	5.18±0.12
pK_B[b]	4.78	4.78	4.78	4.45	4.45	4.45	4.50	4.50	4.58	4.88	4.88	4.88
Logα[c]	2.94±0.20	1.60±0.09	1.37±0.12	0.64±0.46	1.06±0.08	NM	2.58±0.25	2.11±0.12	1.62±0.20	2.74±0.25	2.49±0.15	2.36±0.15
Logτ_B[d]	1.18±0.09	-0.46±0.12	-0.31±0.12	0.14±0.14	-3	NM	1.15±0.09	0.07±0.05	-0.36±0.14	1.75±0.06	0.78±0.05	0.14±0.07

NM; no modulation (NAL effect)

[a]Negative logarithm of the ACh EC_{50} value

[b]Negative logarithm of the binding affinity value determined previously in Mistry et al., (2016), and constrained as a constant in the current analysis.

[c]Logarithm of the cooperativity between ACh and the allosteric modulator, derived using Eqn 2.

[d]Logarithm of the operational efficacy parameter of the allosteric modulator, derived using Eqn 2; or constrained to -3 where no intrinsic efficacy of the allosteric modulator was observed.

FIGURE 1

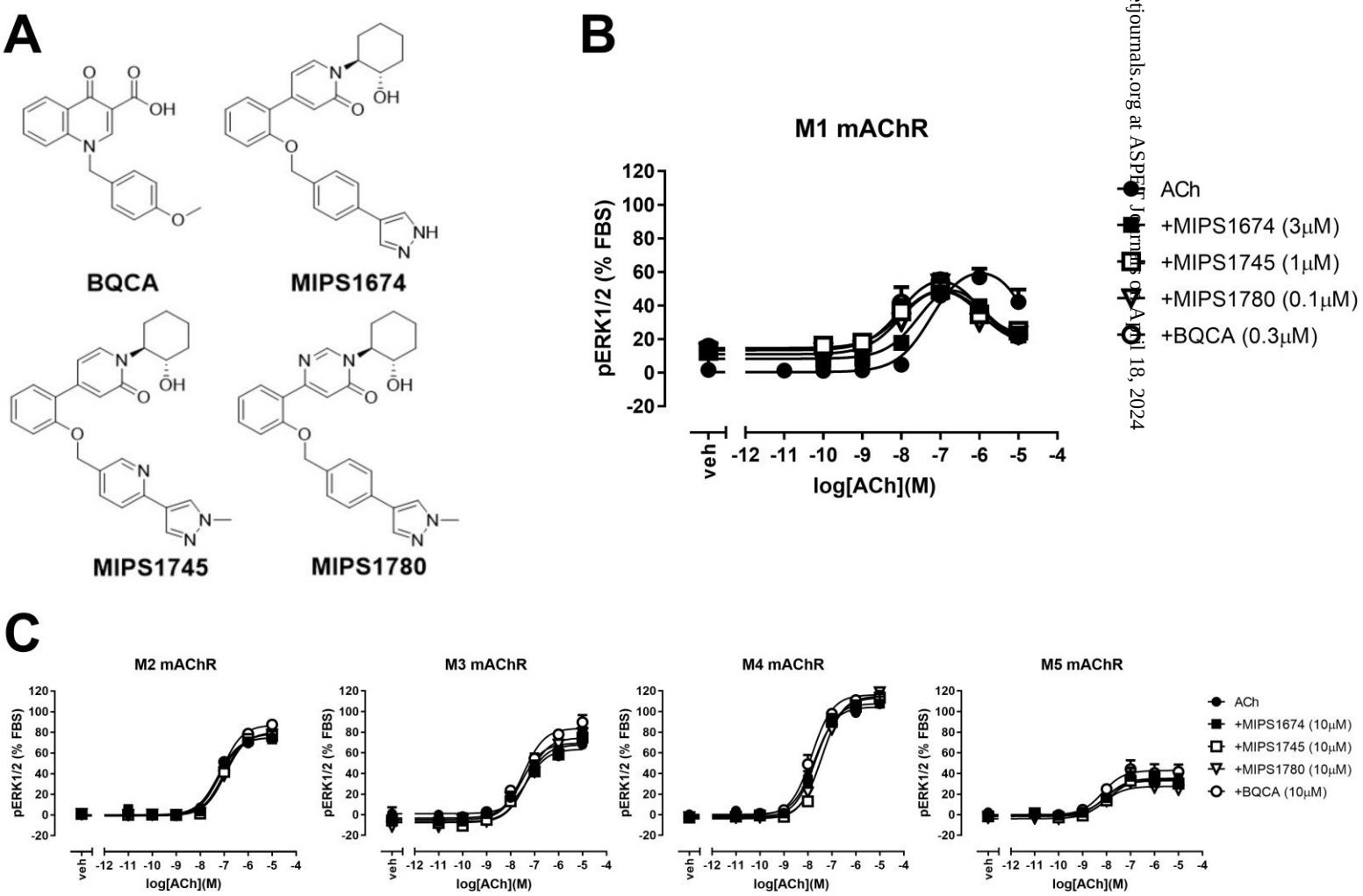

FIGURE 2

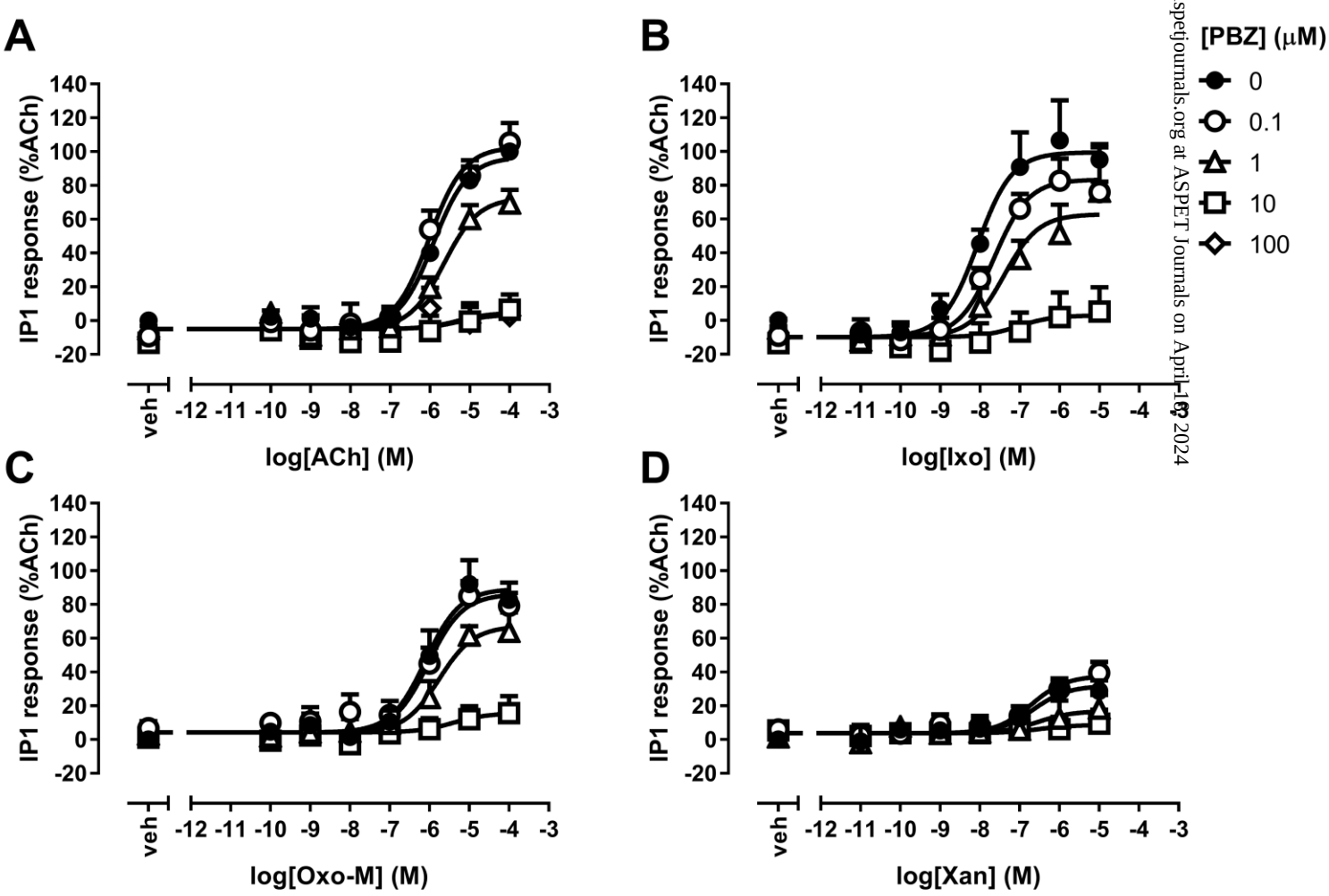

Molecular Pharmacology Fast Forward. Published on April 24, 2018 as DOI: 10.1124/mol.118.111633
This article has not been copyedited and formatted. The final version may differ from this version.

FIGURE 3

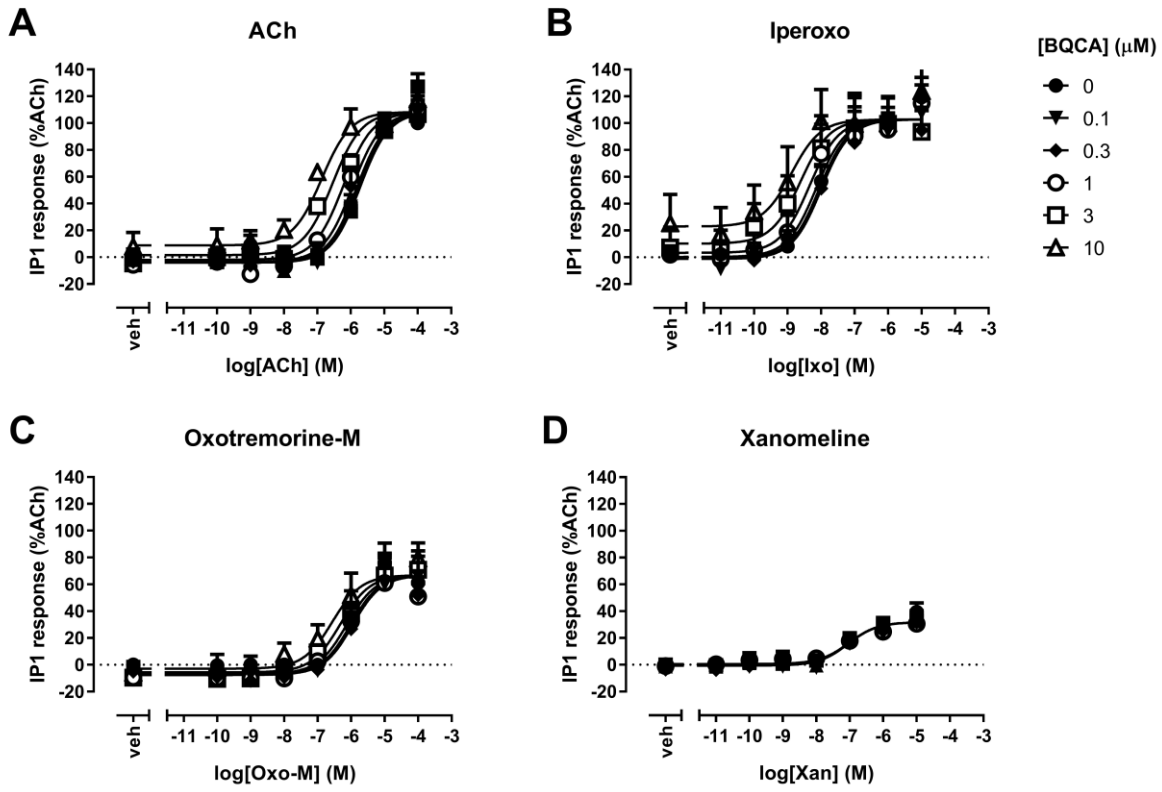

Molecular Pharmacology Fast Forward. Published on April 24, 2018 as DOI: 10.1124/mol.118.111633
This article has not been copyedited and formatted. The final version may differ from this version.

FIGURE 4

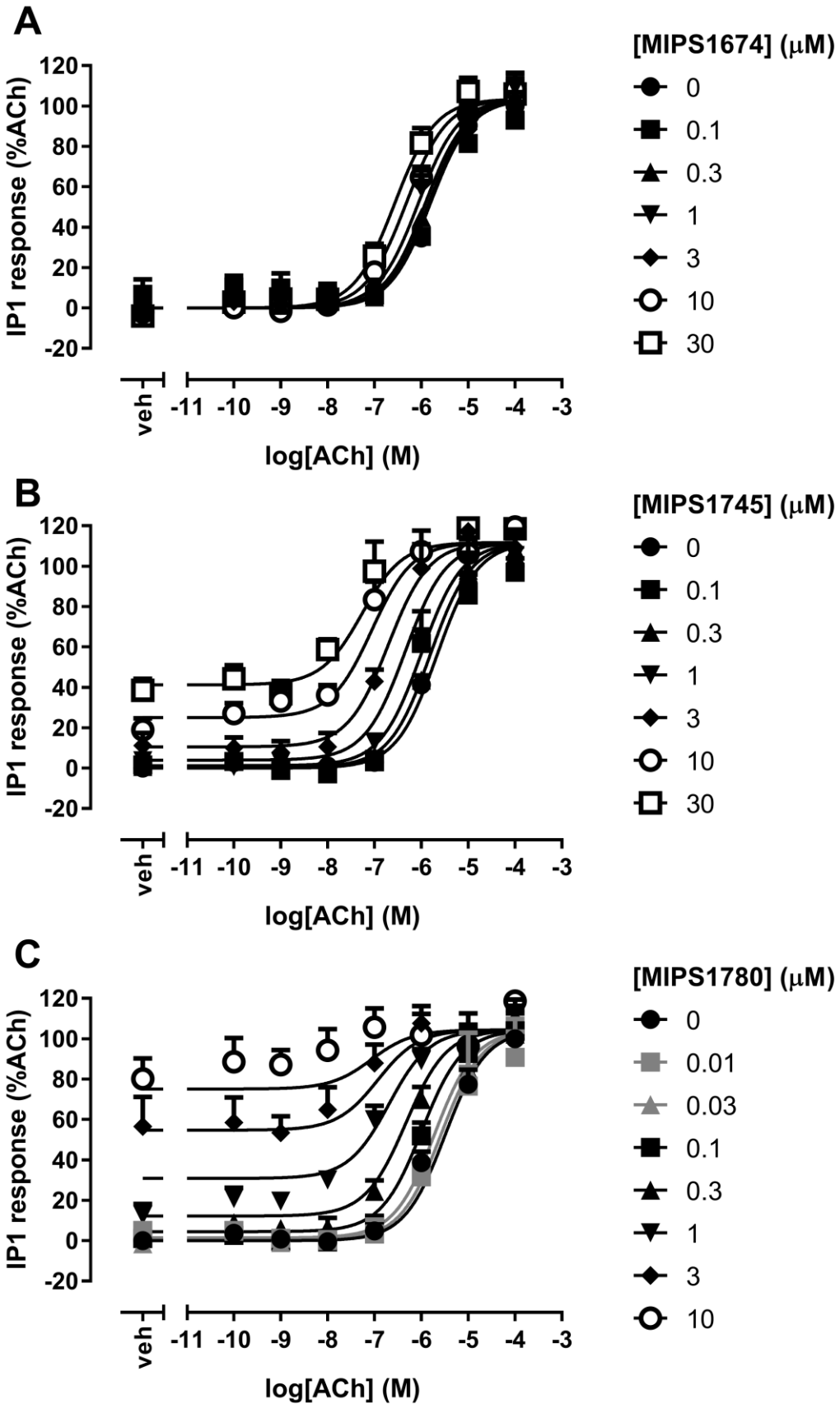

FIGURE 5

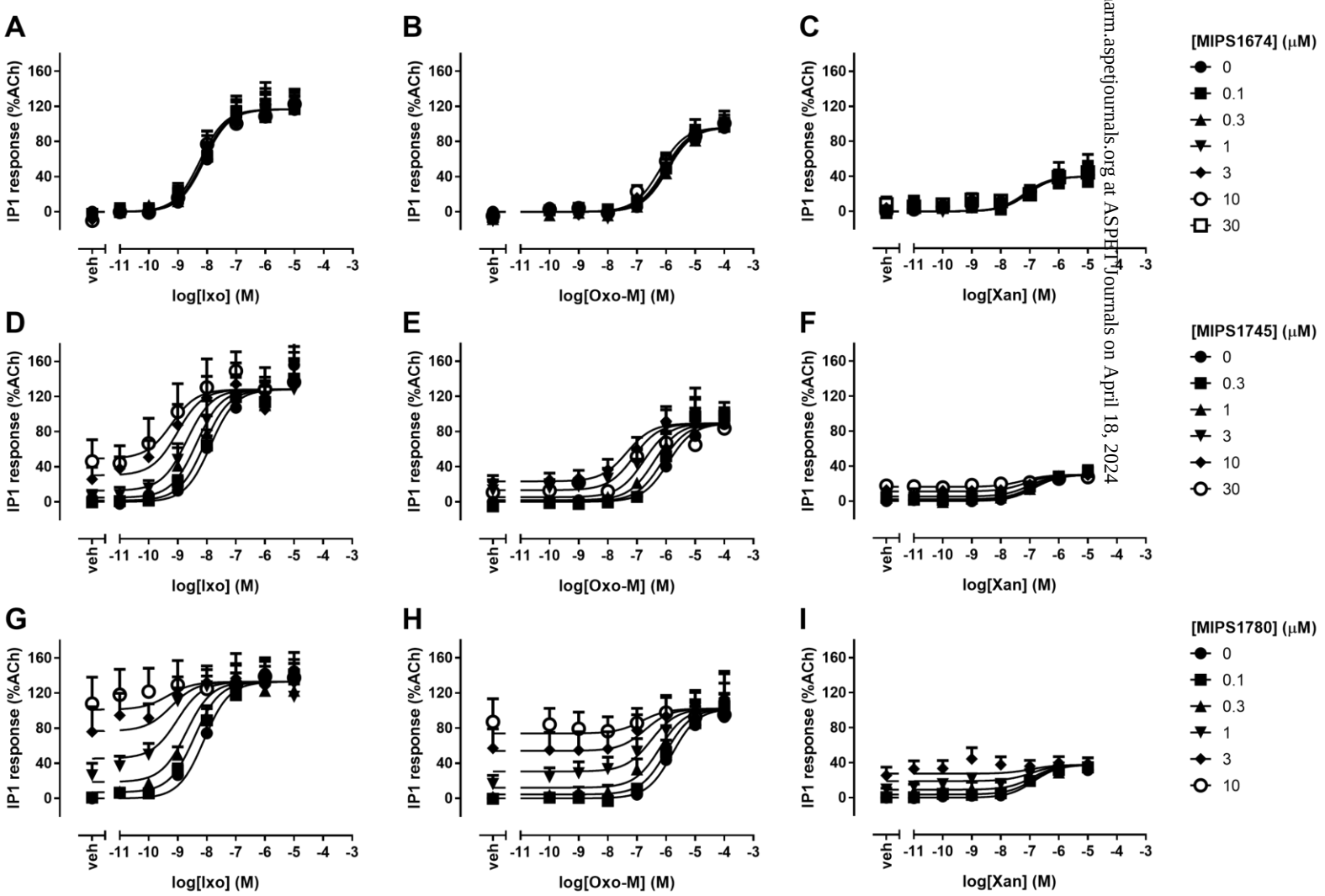

Molecular Pharmacology Fast Forward. Published on April 24, 2018 as DOI: 10.1124/mol.118.111633
This article has not been copyedited and formatted. The final version may differ from this version.

FIGURE 6

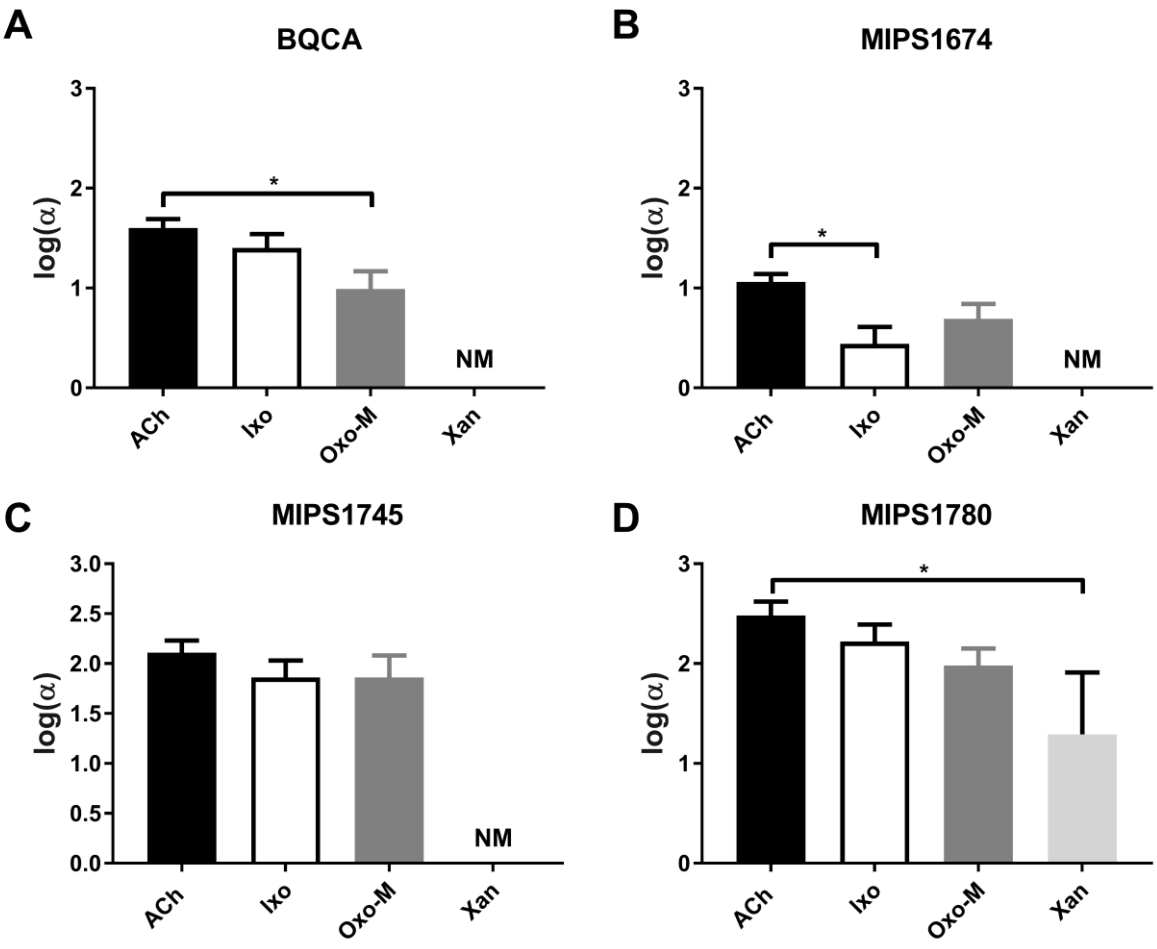

Molecular Pharmacology Fast Forward. Published on April 24, 2018 as DOI: 10.1124/mol.118.111633
This article has not been copyedited and formatted. The final version may differ from this version.

FIGURE 7

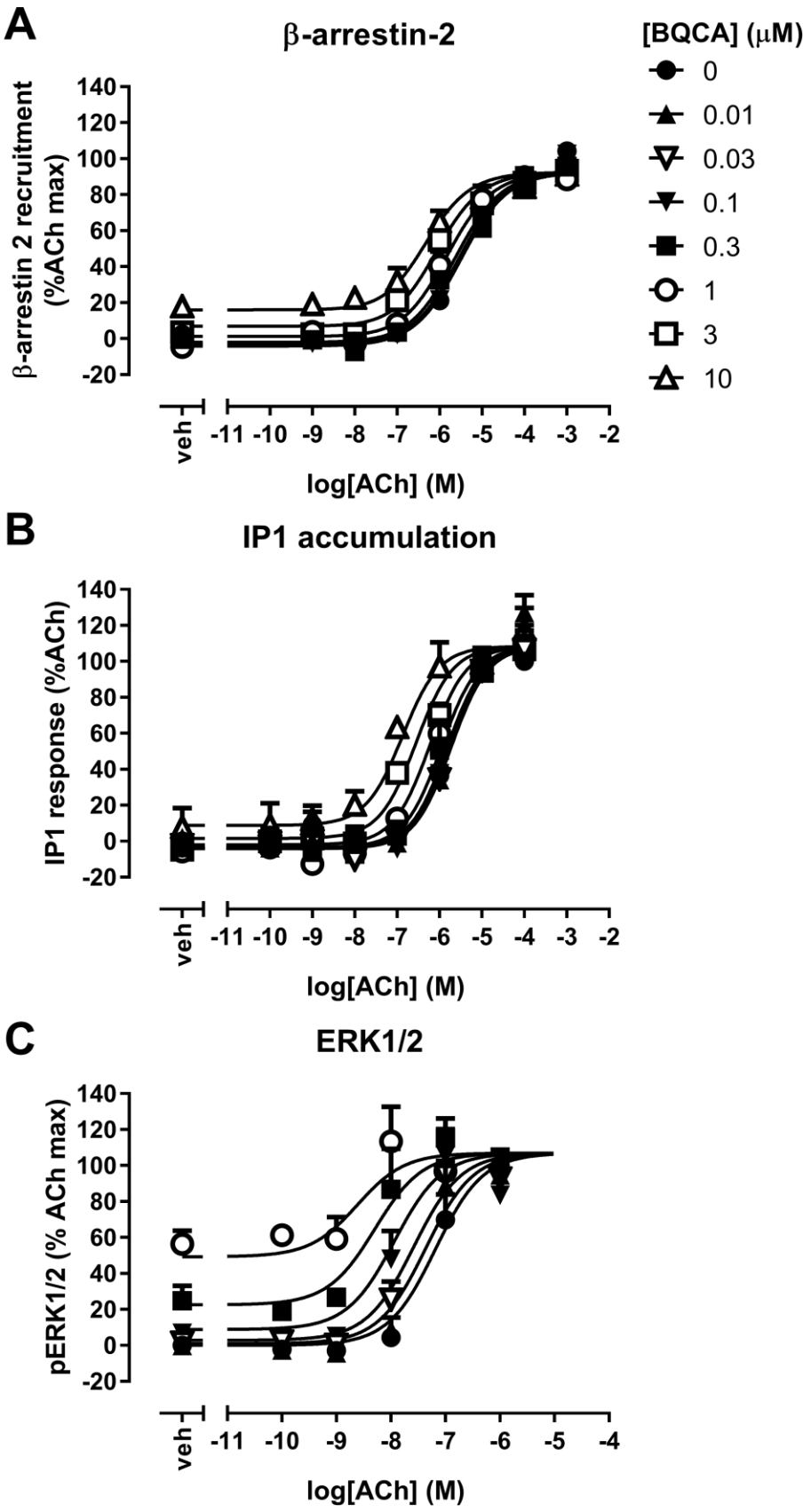

FIGURE 8

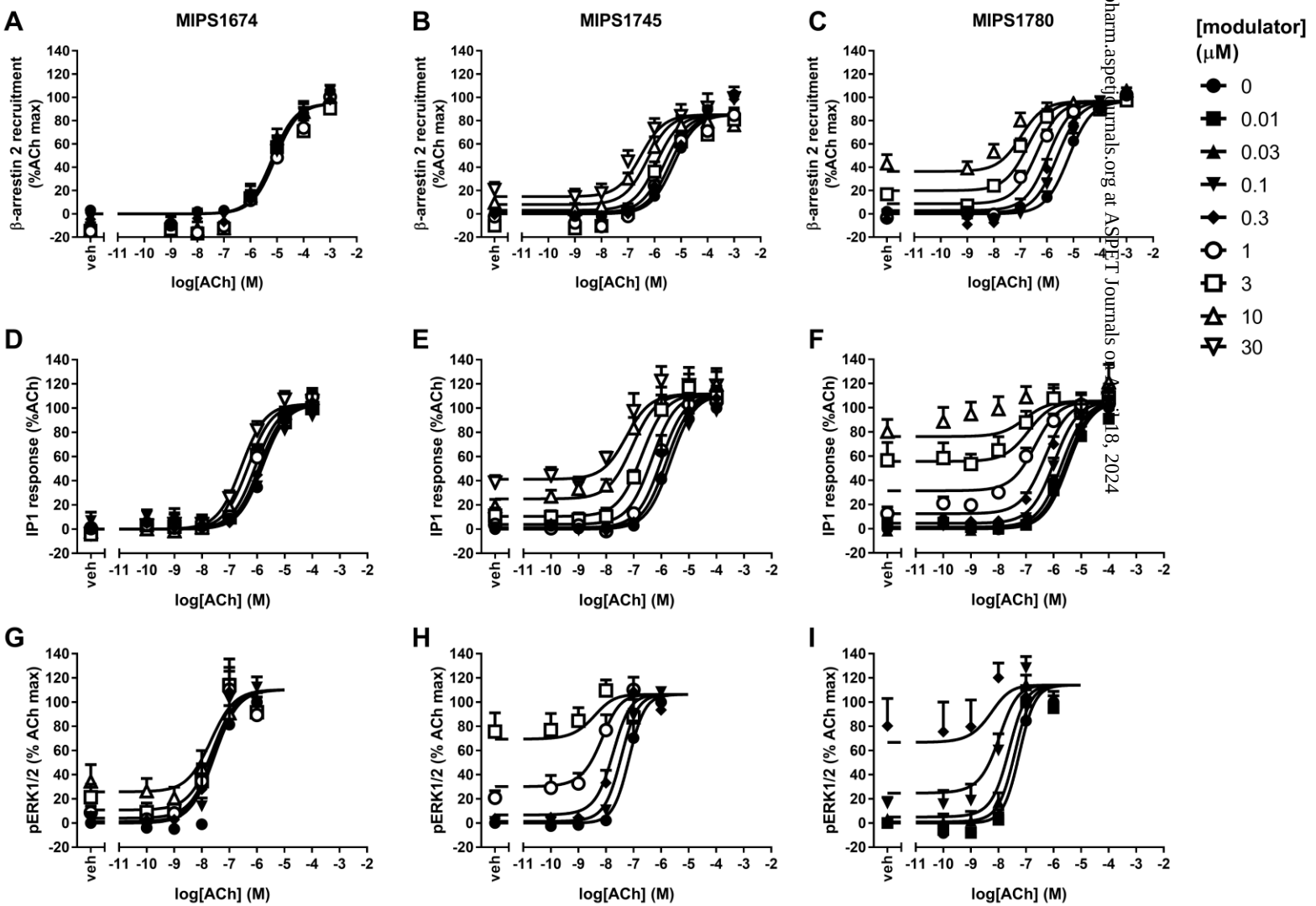

Molecular Pharmacology Fast Forward. Published on April 24, 2018 as DOI: 10.1124/mol.118.111633
This article has not been copyedited and formatted. The final version may differ from this version.

FIGURE 9